10.24425/acs.2019.127530

Archives of Control Sciences
Volume 29(LXV), 2019
No. 1, *pages 169–199*

Sliding mode tracking control for unmanned helicopter using extended disturbance observer

IHSAN ULLAH and HAI-LONG PEI

This paper presents a robust control technique for small-scale unmanned helicopters to track predefined trajectories (velocities and heading) in the presence of bounded external disturbances. The controller design is based on the linearized state-space model of the helicopter. The multivariable dynamics of the helicopter is divided into two subsystems, longitudinal-lateral and heading-heave dynamics respectively. There is no strong coupling between these two subsystems and independent controllers are designed for each subsystem. The external disturbances and model mismatch in the longitudinal-lateral subsystem are present in all (matched and mismatched) channels. This model mismatch and external disturbances are estimated as lumped disturbances using extended disturbance observer and an extended disturbance observer based sliding mode controller is designed for it to counter the effect of these disturbances. In the case of heading-heave subsystem, external disturbances and model mismatch only occur in matched channels so a second order sliding mode controller is designed for it as it is insensitive to matched uncertainties. The control performance is successfully tested in Simulink.

Key words: unmanned helicopter, external disturbances, sliding mode control, extended disturbance observer, mismatched uncertainty

1. Introduction

Miniature helicopters are highly unstable, agile, nonlinear under-actuated system with significant inter-axis dynamic coupling. They are considered to be much more unstable than fixed-wing unmanned air vehicles (UAVs), and constant control action is required at all times. However, a helicopter is a highly flexible aircraft, having the ability to hover, maneuvers accurately and carry heavy loads

Ihsan Ullah (E-mail: a_ihsanullah@yahoo.com) and Hai-Long Pei (Corresponding author, E-mail: auhlpei@scut.edu.cn) are with School of Automation Science & Engineering, South China University of Technology, Guangzhou Guangdong 510640, China and Key Lab of Autonomous Systems and Networked Control, Ministry of Education,Guangzhou, Guangdong 510640, China and Unmanned System Engineering Center of Guangdong Province, China.

This work is supported in part by the Scientific Instruments Development Program of National Natural Science Foundation of China (NSFC) under grant 615278010 and the Science & Technology Planning Project of Guangdong, China under grant 2017B010116005.

Received 27.11.2018.. Revised 02.03.2019.

relative to its own weight [1]. Fixed-wing aircraft are used for application in favorable non-hostile conditions but in adverse condition, agile miniature helicopters become a necessity. The conditions where a helicopter can perform better than fixed-wing UAVs include military investigation, bad weather, firefighting, search and rescue, accessing remote locations and ship operations. In such conditions, helicopters are subjected to unknown external disturbances such as wind and ground effect. These external disturbances have a significant opposing effect on helicopter stability and can have disastrous results in extreme cases. So it is essential to design a controller for the helicopter which can efficiently reject the effects of these unknown external disturbances.

In last two decades, there is substantial research about helicopter control problem. Early results showed that classical control methods using Single-Input Single-Output feedback loops for each input exhibit moderate performance since they are unable to coup with the highly coupled multivariable dynamics of the helicopter [2]. Control schemes typically used to maintain stable control of helicopters include PID [3], Linear Quadratic Regulator (LQR) and Linear Quadratic Gaussian (LQG) [4], H2 [5], H∞ [6] and μ-synthesis [7]. To development a flight control system for a robotic helicopter in [8] a mixing of system identification and multivariable H∞ loop shaping control techniques are applied. An interesting comparative study of several control methods is given in [9, 10]. The majority of linear controllers designed for unmanned helicopter are based on the H∞ method. These linear control methods guarantee stability and robustness only when the system states are near equilibrium but during the flight operations as the speed is increased these methods start losing tracking accuracy significantly. In [11] backstepping control design techniques is used for linear tracking control of miniature helicopter without considering external disturbances, the control design is based on the linearized model of helicopter and shows good results in X-plane flight simulator. Disturbance Observer-based control techniques are used in [12, 13], but in presence of external disturbances, there is steady state error in helicopter rotational and translational dynamics.

Sliding mode control (SMC) is an efficient famous control technique for systems affected by parametric uncertainties and external disturbances having a number of applications in various fields [14]. The traditional SMC method is insensitivity to matched uncertainties and disturbances but many practical systems like the permanent magnet synchronous motors [15], missiles [16, 17] and helicopter [18] are affected by mismatched uncertainties. In these systems parametric uncertainties, un-modeled dynamics and external disturbances affect the states of the system directly rather than through the input channels. Integral sliding mode control (I-SMC) [19] have been proposed in the literature to handle mismatched uncertainties. Although I-SMC is a simple technique and applied to various systems [20, 21], it has disadvantages, such as longer settling time and large overshoots. A novel disturbance observer based sliding mode control

(DOB-SMC) method is proposed in [22] which employ disturbance observer (DO) to cancel the effect of the mismatched uncertainties acting on the system using a modified sliding surface which includes estimation of the mismatched uncertainties. Along with handling the effect of mismatched uncertainties, DOB-SMC also significantly reduces chatter in control but the results are based on the assumption that the mismatched uncertainties and their first derivatives are bounded and the first derivatives go to zero in the steady state. In case of a helicopter, this assumption is very restrictive and the external wind disturbances acting on the helicopter is very complex and can be a function of the power of time t. In [23] an extended disturbance observer based sliding mode control (EDOB-SMC) technique is developed for single-input single-output systems to handle higher order mismatched uncertainties.

In this paper, a simplified EDOB-SMC is proposed for small-scale unmanned helicopters to track predefined velocities trajectories in the presence of bounded external disturbances. The controller design is based on the linearized state-space model of the helicopter. As in [11, 24, 25] the linearized model of the helicopter can be divided into two subsystems, such as the longitudinal-lateral subsystem and the heading-heave subsystem as there is no strong coupling between the two subsystems. The mismatched uncertainties are only present in longitudinal-lateral subsystem while in head-heave subsystem the external disturbances enter the system only through the control input channels. To counteract both matched and mismatched uncertainties in longitudinal-lateral subsystem a new sliding surface augmented with the disturbance estimations of EDOB is designed. The model mismatch and external distances are estimated as lumped disturbances and are compensated in the controller design. As mismatched uncertainties are absent in head-heave subsystem, a 2nd order super-twisting sliding mode controller (ST-SMC) is designed for it. ST-SMC is robust against matched uncertainties and helps reduce control chatter. The rotor flapping dynamics are approximated by the steady-state dynamics of the main rotor which help reducing controller order. The proposed control method has three attractive features. First, it is insensitive to mismatched uncertainties. Second, the chattering problem is substantially reduced as the switching gain is only required to be greater than the bound on the disturbance estimation error of observer instead of lumped disturbance. Third, the proposed controller has better tracking performance than an I-SMC. Simulink simulation has demonstrated successful performance of the proposed controller.

The rest of the paper is organized as follows. A complete nonlinear model of the helicopter and the linearized model for controllers design are presented in section 2. The control problem is stated in section 3. The proposed control laws for longitudinal-lateral and head-heave subsystem are derived in details in section 4 and 5 respectively. Simulation results are given in section 6 and finally concluding remarks are given in section 7.

2. Helicopter model

2.1. Nonlinear dynamics of helicopter

The general 11th state nonlinear model [26] of the miniature unmanned helicopter is given as

$$
\begin{aligned}
\dot{u} &= vr - wq - g\sin\theta + X_{mr}/m + d_{w1},\\
\dot{v} &= wp - ur + g\sin\phi\cos\theta + Y_{mr}/m + d_{w2},\\
\dot{w} &= uq - vp + g\cos\phi\cos\theta + Z_{mr}/m + d_{w3},\\
\dot{\phi} &= p + (\sin\phi\tan\theta)\, q + (\cos\phi\tan\theta)\, r,\\
\dot{\theta} &= (\cos\phi)\, q - (\sin\phi)\, r,\\
\dot{\psi} &= \sin\phi/\cos\theta + \cos\phi/\cos\theta,\\
\dot{p} &= qr\left(I_{yy} - I_{zz}\right)/I_{xx} + L_{mr}/I_{xx} + d_{w4},\\
\dot{q} &= pr\left(I_{zz} - I_{xx}\right)/I_{yy} + M_{mr}/I_{yy} + d_{w5},\\
\dot{r} &= N_v v + N_p p + N_w w + N_r r + N_{ped}.u_{ped} + N_{col}.u_{col} + d_{mm} + d_{w6},\\
\dot{a} &= -q - 1/t_f.a + A_b.b + A_{lon}.u_{lon} + A_{lat}.u_{lat},\\
\dot{b} &= -p - 1/t_f.b + B_a.a + B_{lon}.u_{lon} + B_{lat}.u_{lat},
\end{aligned}
\tag{1}
$$

where $\mathbf{x} = [u\ \ v\ \ w\ \ \phi\ \ \theta\ \ \psi\ \ p\ \ q\ \ r\ \ a\ \ b]^T$ is the vector of state variable all available for measurement except a and b; u, v and w represents linear velocities in longitudinal, lateral and vertical direction respectively; m is mass of helicopter; g represents acceleration due to gravity; p, q and r represents angular velocities in roll, pitch and yaw axis respectively; ϕ, θ and ψ are Euler angles of roll, pitch and yaw axes; $\mathbf{u}_c(t) = \left[u_{lon}\ \ u_{lat}\ \ u_{col}\ \ u_{ped}\right]^T$ is the control input vector; $\mathbf{d}_{wi}\ \forall i = 1, 2, \ldots 6$ are unknown external wind disturbances effecting translational as well as rotational dynamics of helicopter; I_{xx}, I_{yy} and I_{zz} are the rolling moment of inertia, pitching moment of inertia and yawing moment of inertia respectively; a and b are flapping angles of tip-path-plane(TPP) in longitudinal and lateral direction respectively; X_{mr}, Y_{mr} and Z_{mr} are the force components of main rotor trust along x, y and z axis; L_{mr} and M_{mr} are roll and pitch moments generated by main rotor; N_v, N_p, N_w and N_r are helicopter stability derivatives and N_{ped} and N_{col} are input derivatives of yaw dynamics identified as in [11]; t_f is flapping time constant; B_a, B_{lat} and B_{lon} are lateral flapping derivatives; A_b, A_{lon} and A_{lat} are longitudinal flapping derivatives. A diagram showing the directions of the helicopter body fixed coordinate system is given in Fig. 1.

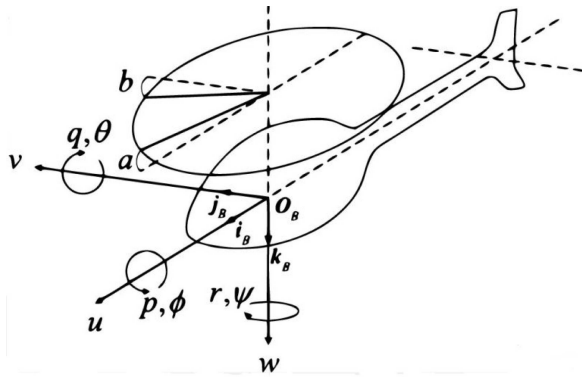

Figure 1: Helicopter body-fixed coordinate system [11]

The force components generated by the main rotor trust in x, y and z direction are given as

$$\begin{aligned} X_{mr} &= -T\sin a, \\ Y_{mr} &= T\sin b, \\ Z_{mr} &= -T\cos a\cos b, \end{aligned} \tag{2}$$

where T is the total trust generated by the main rotor. The moments generated by the main rotor along the x and y direction are calculated as

$$\begin{aligned} L_{mr} &= \left(k_\beta + T.h_{mr}\right)\sin b, \\ M_{mr} &= \left(k_\beta + T.h_{mr}\right)\sin a \end{aligned} \tag{3}$$

where k_β is the torsional stiffness of the main rotor hub; h_{mr} is main rotor hub height above the center of gravity of helicopter.

The trust of the main rotor is calculated by iteratively solving the equations of trust and the induced inflow velocity [27].

$$\begin{aligned} T &= (w_b - v_i)\,\frac{\rho\Omega R^2 C_{l\alpha}^m b_m c_m}{4}, \\ v_i^2 &= \sqrt{\left(\frac{\bar{v}^2}{2}\right)^2 + \left(\frac{T}{2\rho\pi R^2}\right)^2} - \frac{\bar{v}^2}{2}, \\ \bar{v}^2 &= u^2 + v^2 + w(w - 2v_i), \\ w_b &= w + \frac{2}{3}\Omega R k_a k_{col} u_{col}, \end{aligned} \tag{4}$$

where v_i is the induced inflow velocity; Ω is rotational speed of the main rotors; ρ is air density; R is main rotor radius; b_m is the number of main rotor blades; c_m is the chord length of the main rotor; $C_{l\alpha}^m$ is coefficient of lift curve slope of the main rotor; is control gain of the servo actuator; k_{col} is linkage gain from the collective actuator to the main blade.

2.2. Linearized State Space Model of the helicopter

To derive the control law, the nonlinear model (1) of the helicopter is linearized at hover condition as

$$\begin{aligned} \dot{\mathbf{x}} &= A\mathbf{x} + B\mathbf{u}_c + E\mathbf{d}_t, \\ \mathbf{y} &= C\mathbf{x}. \end{aligned} \tag{5}$$

At hover condition, the longitudinal-lateral and heading-heave dynamics of the helicopter are weakly coupled with each other and are expressed as two separate sub-systems [11].

$$\begin{aligned} \dot{\mathbf{x}}_1 &= A_{11}\mathbf{x}_1 + B_{11}\mathbf{u}_{c1} + E_{11}\mathbf{d}_{t1}, \\ \mathbf{y}_1 &= C_1\mathbf{x}_1; \end{aligned} \tag{6}$$

$$\begin{aligned} \dot{\mathbf{x}}_2 &= A_{21}\mathbf{x}_1 + A_{22}\mathbf{x}_2 + B_{22}\mathbf{u}_{c2} + E_{22}\mathbf{d}_{t2}, \\ \mathbf{y}_2 &= C_2\mathbf{x}_2, \end{aligned} \tag{7}$$

where (6) represents longitudinal-lateral subsystem and (7) represents the heading-heave subsystem, $\mathbf{x}_1 = [u \;\; v \;\; \theta \;\; \phi \;\; q \;\; p \;\; a \;\; b]^T$; $\mathbf{u}_{c1} = [u_{lon} \;\; u_{lat}]^T$; $\mathbf{d}_{t1} = [d_{t1} \;\; d_{t2} \;\; d_{t3} \;\; d_{t4} \;\; d_{t5} \;\; d_{t6} \;\; 0 \;\; 0]^T$; E_{11} is an 8×8 identity matrix; $\mathbf{x}_2 = [\psi \;\; r \;\; w]^T$; $\mathbf{u}_{c2} = \left[u_{ped} \;\; u_{col}\right]^T$; $\mathbf{d}_{t2} = [0 \;\; d_{t7} \;\; d_{t8}]^T$; E_{11} is 3×3 identity matrix; Matrices A_{11}, A_{21}, A_{22}, B_{11}, B_{22}, C_1, C_2 are given as

$$A_{11} = \begin{bmatrix} X_u & 0 & -g & 0 & 0 & 0 & 0 & 0 \\ 0 & Y_v & 0 & g & 0 & 0 & 0 & 0 \\ 0 & 0 & 0 & 0 & 1 & 0 & 0 & 0 \\ 0 & 0 & 0 & 0 & 0 & 1 & 0 & 0 \\ M_u & M_v & 0 & 0 & 0 & 0 & M_a & 0 \\ L_u & L_v & 0 & 0 & 0 & 0 & 0 & L_b \\ 0 & 0 & 0 & 0 & -1 & 0 & -1/t_f & A_b \\ 0 & 0 & 0 & 0 & 0 & -1 & B_a & -1/t_f \end{bmatrix}, \tag{8a}$$

$$B_{11} = \begin{bmatrix} 0 & 0 \\ 0 & 0 \\ 0 & 0 \\ 0 & 0 \\ 0 & 0 \\ 0 & 0 \\ A_{lon} & A_{lat} \\ B_{lon} & B_{lat} \end{bmatrix}, \qquad C_1 = \begin{bmatrix} 1 & 0 \\ 0 & 1 \\ 0 & 0 \\ 0 & 0 \\ 0 & 0 \\ 0 & 0 \\ 0 & 0 \\ 0 & 0 \end{bmatrix}^T \tag{8b}$$

$$A_{21} = \begin{bmatrix} 0 & 0 & 0 & 0 & 0 & 0 & 0 & 0 \\ 0 & N_v & 0 & 0 & 0 & N_p & 0 & 0 \\ 0 & 0 & 0 & 0 & 0 & 0 & Z_a & Z_b \end{bmatrix}, \qquad C_2 = \begin{bmatrix} 1 & 0 \\ 0 & 0 \\ 0 & 1 \end{bmatrix},$$
$$A_{22} = \begin{bmatrix} 0 & 1 & 0 \\ 0 & N_r & N_w \\ 0 & Z_r & Z_w \end{bmatrix}, \qquad B_{22} = \begin{bmatrix} 0 & 0 \\ N_{ped} & N_{col} \\ 0 & Z_{col} \end{bmatrix}. \tag{9}$$

Assumption 1 *The matrix pairs* (A_{11}, B_{11}) *and* (A_{22}, B_{22}) *are controllable [11].*

Assumption 2 *Each matrix* B_{11} *and* B_{22} *have two linearly independent rows [11].*

Assumption 3 *The stability derivatives* g, M_a *and* L_b *are nonzero [11].*

Assumptions 1, 2 and 3 reflect the fact that the linearized models (6) and (7) are physically meaningful.

Assumption 4 *The disturbances* d_{ti}, $\forall\ i = 1, 2, \ldots, 6$ *acting at the system (6) are continuous and satisfy*

$$\left| d^j(d_{ti}) \Big/ dt^j \right| \leqslant \mu_{ij} \ \forall \ \ i = 1, 2, \ldots, 6 \ \ \text{and} \ \ j = 0, 1, 2, 3 \tag{10a}$$

and let

$$\mu_j = \left\| \mu_{1j} \quad \mu_{2j} \quad \mu_{3j} \quad \mu_{4j} \quad \mu_{5j} \quad \mu_{6j} \right\|_2, \tag{10b}$$

where all μ_{ij} *and* μ_j *are positive bounded constant.*

Assumption 5 *The disturbances acting at the subsystem (7) are also continuous and satisfies*

$$\left| d^j(d_{ti}) \Big/ dt^j \right| \leqslant \mu_{ij} \quad for \ \ i = 7, 8 \ \ and \ \ j = 0, 1, \tag{11}$$

where μ_{ij} *is positive bounded constant.*

3. Control problem statement

The principal objective of this paper is to derive the control laws $\mathbf{u}_{c1}$ and $\mathbf{u}_{c2}$ for the helicopter system (1) to follow a predefined reference velocity trajectory $\mathbf{v}_r = [u_r \;\; v_r \;\; w_r]^T$ and yaw angle (ψ_r), in presence of external wind disturbances satisfying assumption 4. As subsystem (6) and (7) are decoupled, separate controllers are designed for each subsystem in the following sections.

Assumption 6 *The desired reference velocities and yaw angle are continuous and bounded such that* $\frac{d^i}{dt}(u_r)$, $\frac{d^i}{dt}(v_r) \in L_\infty$ $(i = 0, 1, 2, 3,)$ *and* $\frac{d^i}{dt}(w_r)$, $\frac{d^i}{dt}(\psi_r) \in L_\infty$ $(i = 0, 1)$.

4. Longitudinal-lateral subsystem

The subsystem (6) is expanded as

$$\begin{aligned}
\dot{u} &= X_u u - g\theta + d_{t1},\\
\dot{v} &= Y_v v + g\phi + d_{t2},\\
\dot{\theta} &= q + d_{t3},\\
\dot{\phi} &= p + d_{t4},\\
\dot{q} &= M_u u + M_v v + M_a a + d_{t5},\\
\dot{p} &= L_u u + L_v v + L_b b + d_{t6},\\
\dot{a} &= -q - 1/t_f.a + A_b.b + A_{lon}.u_{lon} + A_{lat}.u_{lat},\\
\dot{b} &= -p - 1/t_f.b + B_a.a + B_{lon}.u_{lon} + B_{lat}.u_{lat},
\end{aligned} \tag{12}$$

$$y_1 = [u \quad v]^T, \tag{13}$$

where X_u, Y_v, M_u, M_v, M_a, L_u, L_v and L_b are stability derivatives; A_{lon}, A_{lat}, B_{lon} and B_{lat} are input derivatives; d_{ti} $\forall\, i = 1, 2, \cdots, 6$ is the total disturbance including both model mismatch and external disturbances acting at channel i.

The flapping angles a and b of the main rotor can be approximated by the steady state dynamics of the main rotor as in [28]

$$a = -t_f q + t_f (A_b.b + A_{lon}.u_{lon} + A_{lat}.u_{lat}), \tag{14}$$

$$b = -t_f p + t_f (B_a.a + B_{lon}.u_{lon} + B_{lat}.u_{lat}). \tag{15}$$

Solving (14) and (15) for a and b and then substituting it in (12) gives the reduced order linearized model for the longitudinal-lateral systems as

$$\begin{aligned}
\dot{u} &= X_u u - g\theta + d_{t1},\\
\dot{v} &= Y_v v + g\phi + d_{t2},\\
\dot{\theta} &= q + d_{t3},\\
\dot{\phi} &= p + d_{t4},\\
\dot{q} &= M_u u + M_v v - M_p p - M_q q + M_{lon}.u_{lon} + M_{lat}.u_{lat} + d_{t5},\\
\dot{p} &= L_u u + L_v v - L_p p - L_q q + L_{lon}.u_{lon} + L_{lat}.u_{lat} + d_{t6}.
\end{aligned} \tag{16}$$

The reduced order linearized model (16) is written in state space form as follows

$$\dot{\mathbf{x}}_r = A_r \mathbf{x}_r + B_r \mathbf{u}_{c1} + E_r \mathbf{d}_{tr}, \tag{17}$$

$$\mathbf{y}_1 = C_r \mathbf{x}_r, \tag{18}$$

where $\mathbf{x}_r = [u \;\; v \;\; \theta \;\; \phi \;\; q \;\; p]^T$; $\mathbf{u}_{c1} = [u_{lon} \;\; u_{lat}]^T$; $\mathbf{d}_{tr} = [d_{t1} \; d_{t2} \; d_{t3} \; d_{t4} \; d_{t5} \; d_{t6}]^T$; E_r is 6×6 identity matrix; $\mathbf{y}_r$ is output vector; Matrices A_r, B_r and C_r are given as

$$A_r = \begin{bmatrix} X_u & 0 & -g & 0 & 0 & 0\\ 0 & Y_v & 0 & g & 0 & 0\\ 0 & 0 & 0 & 0 & 1 & 0\\ 0 & 0 & 0 & 0 & 0 & 1\\ M_u & M_v & 0 & 0 & -M_q & -M_p\\ L_u & L_v & 0 & 0 & -L_q & -L_p \end{bmatrix}, \quad B_r = \begin{bmatrix} 0 & 0\\ 0 & 0\\ 0 & 0\\ 0 & 0\\ M_{lon} & M_{lat}\\ L_{lon} & L_{lat} \end{bmatrix}, \quad C_r = \begin{bmatrix} 1 & 0\\ 0 & 1\\ 0 & 0\\ 0 & 0\\ 0 & 0\\ 0 & 0 \end{bmatrix}^T.$$

4.1. Extended disturbance observer design

It is difficult to measure directly the disturbance vector $\mathbf{d_{tr}}$ and its higher derivatives, a 3rd order EDO is used to estimate the unknown total disturbance vector $\mathbf{d}_{tr}$ and its higher derivatives. The observer is designed as

$$\dot{\mathbf{P}}_1 = -L_1(\mathbf{P}_1 + L_1\mathbf{x}_r) - L_1(A_r\mathbf{x}_r + B_r\mathbf{u}_{c1}) + \hat{\dot{\mathbf{d}}}_{tr}, \tag{19a}$$

$$\hat{\mathbf{d}}_{tr} = \mathbf{P}_1 + L_1\mathbf{x}_r, \tag{19b}$$

$$\dot{\mathbf{P}}_2 = -L_2(\mathbf{P}_1 + L_1\mathbf{x}_r) - L_2(A_r\mathbf{x}_r + B_r\mathbf{u}_{c1}) + \hat{\ddot{\mathbf{d}}}_{tr}, \tag{20a}$$

$$\hat{\dot{\mathbf{d}}}_{tr} = \mathbf{P}_2 + L_2\mathbf{x}_r, \tag{20b}$$

$$\dot{\mathbf{P}}_3 = -L_3(\mathbf{P}_1 + L_1\mathbf{x}_r) - L_3(A_r\mathbf{x}_r + B_r\mathbf{u}_{c1}), \tag{21a}$$

$$\hat{\ddot{\mathbf{d}}}_{tr} = \mathbf{P}_3 + L_3\mathbf{x}_r, \tag{21b}$$

where $\mathbf{P}_1$, $\mathbf{P}_2$ and $\mathbf{P}_3$ are auxiliary state vectors of the observer; $\hat{\mathbf{d}}_{tr}$, $\dot{\hat{\mathbf{d}}}_{tr}$ and $\ddot{\hat{\mathbf{d}}}_{tr}$ are estimation of the disturbance vector $\mathbf{d}_{tr}$ and its higher derivatives; L_1, L_2 and L_3 are observer gains defined as

$$L_i = l_i I_{6\times 6} \quad \text{for} \quad i = 1,2,3. \tag{22}$$

The observer estimation error vector is defined as

$$\mathbf{e} = \begin{bmatrix} \mathbf{e_d} & \mathbf{e_{\dot{d}}} & \mathbf{e_{\ddot{d}}} \end{bmatrix}, \tag{23}$$

where

$$\mathbf{e_d} = \hat{\mathbf{d}}_{tr} - \mathbf{d}_{tr} = [e_{dt1} \quad e_{dt2} \quad e_{dt3} \quad e_{dt4} \quad e_{dt5} \quad e_{dt6}]^T \tag{24a}$$

$$\mathbf{e_{\dot{d}}} = \dot{\hat{\mathbf{d}}}_{tr} - \dot{\mathbf{d}}_{tr} = \begin{bmatrix} e_{\dot{d}t1} & e_{\dot{d}t2} & e_{\dot{d}t3} & e_{\dot{d}t4} & e_{\dot{d}t5} & e_{\dot{d}t6} \end{bmatrix}^T, \tag{24b}$$

$$\mathbf{e_{\ddot{d}}} = \ddot{\hat{\mathbf{d}}}_{tr} - \ddot{\mathbf{d}}_{tr} = \begin{bmatrix} e_{\ddot{d}t1} & e_{\ddot{d}t2} & e_{\ddot{d}t3} & e_{\ddot{d}t4} & e_{\ddot{d}t5} & e_{\ddot{d}t6} \end{bmatrix}^T. \tag{24c}$$

From (19a), (19b) and (17)

$$\dot{\hat{\mathbf{d}}}_{tr} = -L_1 \mathbf{e_d} + \hat{\mathbf{d}}_{tr}. \tag{25}$$

Subtracting both sides of (25) from $\dot{\mathbf{d}}_{tr}$

$$\dot{\mathbf{e}}_{\mathbf{d}} = -L_1 \mathbf{e_d} + \mathbf{e_{\dot{d}}}. \tag{26}$$

Similarly using (20a), (20b), (17) and (21a), (21b), (17) gives

$$\dot{\mathbf{e}}_{\dot{\mathbf{d}}} = -L_2 \mathbf{e_d} + \mathbf{e_{\ddot{d}}}, \tag{27}$$

$$\dot{\mathbf{e}}_{\ddot{\mathbf{d}}} = -L_3 \mathbf{e_d} + \dddot{\mathbf{d}}_{\mathbf{tr}}. \tag{28}$$

Combining (26), (27) and (28) the observer error dynamics is written in compact form as

$$\dot{\mathbf{e}} = D\mathbf{e} + E\dddot{\mathbf{d}}_{\mathbf{tr}}, \tag{29}$$

where

$$D = \begin{bmatrix} -L_1 & I_{6\times 6} & 0_{6\times 6} \\ -L_2 & 0_{6\times 6} & I_{6\times 6} \\ -L_3 & 0_{6\times 6} & 0_{6\times 6} \end{bmatrix}, \qquad E = \begin{bmatrix} 0_{6\times 6} \\ 0_{6\times 6} \\ I_{6\times 6} \end{bmatrix}. \tag{30}$$

If l_1, l_2 and l_3 are selected such that the following equation is Hurwitz

$$s^3 + l_1 s^2 + l_2 s + l_3 = 0 \tag{31}$$

then D is Hurwitz and a positive definite matrix P_1 always exist satisfying the following equation

$$D^T P_1 + P_1 D = -\mathrm{Q}_1. \tag{32}$$

Theorem 1 *If L_1, L_2 and L_3 are chosen such that D is Hurwitz, the estimation error* $\mathbf{e}$ *of the EDOB asymptotically goes inside a ball* $b_0 = \{\mathbf{e} \in R^{18} \mid \mathbf{e} \leqslant 2\mu_3 [\lambda_{\max}(P_1)/\lambda_{\min}(\mathrm{Q}_1)]\}$ *and stays inside for the remaining period of time.*

Proof. Defining the Lyapunov function as

$$V(\mathbf{e}) = \mathbf{e}^T P_1 \mathbf{e}. \tag{33}$$

Differentiating $V(\mathbf{e})$ with respect to time t gives

$$\begin{aligned} \dot{V}(\mathbf{e}) &= \mathbf{e}^T \left(D^T P_1 + P_1 D\right) \mathbf{e} + 2\mathbf{e}^T P_1 E \dddot{\mathbf{d}}_{tr} \\ &\leqslant -\mathbf{e}^T (\mathrm{Q}_1)\, \mathbf{e} + 2\mathbf{e}^T \lambda_{\max}(P_1)\mu_3 \\ &\leqslant -\|\mathbf{e}\| \left[\lambda_{\min}(\mathrm{Q}_1) \|\mathbf{e}\| - 2\lambda_{\max}(P_1)\, \mu_3\right]. \end{aligned} \tag{34}$$

From $\dot{V}(\mathbf{e}) \leqslant 0$, it is concluded that the observer estimation error norm $\|\mathbf{e}\|$ asymptotically converges to b_0 and stay inside for the remaining period of time such that

$$\|\mathbf{e}\| \leqslant 2\mu_3 [\lambda_{\max}(P_1)/\lambda_{\min}(\mathrm{Q}_1)]. \tag{35}$$

□

Assumption 7 *The estimation error of EDOB is bounded such that*

$$e^*_{dti} = \max_{t>0} |e_{dti}| \quad \forall\, i = 1, 2, \cdots, 6. \tag{36}$$

4.2. EDOB-SMC design

4.2.1. Input-output linearization

First, the longitudinal-lateral dynamics (17) is written in input-output linearized form. The system output (18) is expanded as

$$\mathbf{y}_1 = [u \quad v]^T. \tag{37}$$

Differentiating $\mathbf{y}_1$ gives

$$\dot{\mathbf{y}}_1 = K_1 [u \quad v]^T + K_2 [\theta \quad \phi]^T + \mathbf{d}_{tr1}, \tag{38}$$

where $K_1 = \mathrm{diag}\,(X_u, Y_v)$; $K_2 = \mathrm{diag}\,(-g, g)$ and $\mathbf{d}_{tr1} = [d_{t1} \quad d_{t2}]^T$. Differentiating (38) gives

$$\ddot{\mathbf{y}}_1 = K_1^2 [u \quad v]^T + K_1 K_2 [\theta \quad \phi]^T + K_2 [q \quad p]^T + K_1 \mathbf{d}_{tr1} + K_2 \mathbf{d}_{tr2} + \dot{\mathbf{d}}_{tr1}, \tag{39}$$

where $\mathbf{d}_{tr2} = [d_{t3} \quad d_{t4}]^T$. Differentiating (39) gives

$$\begin{aligned}\dddot{\mathbf{y}}_1 &= K_1^3[u \quad v]^T + K_1^2K_2[\theta \quad \phi]^T + K_1K_2[q \quad p]^T + K_2K_3[u_{lon} \quad u_{lat}]^T \\ &+ K_2K_4[u \quad v \quad q \quad p]^T + K_1^2\mathbf{d}_{tr1} + K_1K_2\mathbf{d}_{tr2} + K_2\mathbf{d}_{tr3} + K_1\dot{\mathbf{d}}_{tr1} \\ &+ K_2\dot{\mathbf{d}}_{tr2} + \ddot{\mathbf{d}}_{tr1},\end{aligned} \tag{40}$$

where $\mathbf{d}_{tr3} = \begin{bmatrix} d_{t5} \\ d_{t6} \end{bmatrix}$; $K_3 = \begin{bmatrix} M_{lon} & M_{lat} \\ L_{lon} & L_{lat} \end{bmatrix}$; $K_4 = \begin{bmatrix} M_u & M_v & -M_q & -M_p \\ L_u & L_v & -L_p & -L_q \end{bmatrix}$.

4.2.2. Controller design

In this section EDOB-SMC method is used to derive the control law $\mathbf{u}_{c1}$ for longitudinal and lateral velocities tracking of helicopter in presence of external disturbances. The reference velocity vector is given as

$$\mathbf{y}_r = [u_r \quad v_r]^T. \tag{41}$$

The sliding surface augmented with the estimated disturbances is designed as follows

$$\begin{aligned}\mathbf{S} &= C_1(\mathbf{y}_1 - \mathbf{y}_r) + C_2\left(\hat{\dot{\mathbf{y}}}_1 - \dot{\mathbf{y}}_r\right) + \hat{\ddot{\mathbf{y}}}_1 - \ddot{\mathbf{y}}_r \\ &= C_1\mathbf{e}_y + C_2\hat{\dot{\mathbf{e}}}_y + \hat{\ddot{\mathbf{e}}}_y,\end{aligned} \tag{42}$$

where $\mathbf{S} = [s_1 \quad s_2]^T$; $C_1 = \text{diag}(c_1, c_2)$; $C_2 = \text{diag}(c_3, c_4)$. C_1 and C_2 are designed such that $\mathbf{S} = bf0$ is Hurwitz; $\dot{\mathbf{y}}_r$, $\ddot{\mathbf{y}}_r$ are higher derivatives of $\mathbf{y}_r$; $\hat{\dot{\mathbf{y}}}_1$ and $\hat{\ddot{\mathbf{y}}}_1$ are expressed as follows

$$\hat{\dot{\mathbf{y}}}_1 = K_1[u \quad v]^T + K_2[\theta \quad \phi]^T + \hat{\mathbf{d}}_{tr1}, \tag{43}$$

$$\hat{\ddot{\mathbf{y}}}_1 = K_1^2[u \quad v]^T + K_1K_2[\theta \quad \phi]^T + K_2[q \quad p]^T + K_1\hat{\mathbf{d}}_{tr1} + K_2\hat{\mathbf{d}}_{tr2} + \hat{\dot{\mathbf{d}}}_{tr1}, \tag{44}$$

where $\hat{\mathbf{d}}_{tr1} = \left[\hat{d}_{t1} \quad \hat{d}_{t2}\right]^T$, $\hat{\mathbf{d}}_{tr2} = \left[\hat{d}_{t3} \quad \hat{d}_{t4}\right]^T$ and $\hat{\dot{\mathbf{d}}}_{tr1} = \left[\widehat{\dot{d}}_{t1} \quad \widehat{\dot{d}}_{t2}\right]^T$.

Then the EDOB-SMC is designed as follows

$$\begin{aligned}\mathbf{u}_{c1} = (-K_2K_3)^{-1}\Big(&\mathbf{h} + C_1\hat{\mathbf{d}}_{tr1} + C_2\left(K_1\hat{\mathbf{d}}_{tr1} + K_2\hat{\mathbf{d}}_{tr2}\right) + K_1^2\hat{\mathbf{d}}_{tr1} + K_1K_2\hat{\mathbf{d}}_{tr2} \\ &+ K_2\hat{\mathbf{d}}_{tr3} + (C_2 + K_1)\hat{\dot{\mathbf{d}}}_{tr1} + K_2\hat{\dot{\mathbf{d}}}_{tr2} + \hat{\ddot{\mathbf{d}}}_{tr1} + \beta\text{sgn}(\mathbf{S})\Big),\end{aligned} \tag{45}$$

where $\hat{\dot{\mathbf{d}}}_{tr1} = \left[\hat{\dot{d}}_{t1} \quad \hat{\dot{d}}_{t2}\right]^T$; $\hat{\mathbf{d}}_{tr3} = \left[\hat{d}_{t5} \quad \hat{d}_{t6}\right]^T$; $\text{sgn}(S) = [\text{sgn}(s_1) \quad \text{sgn}(s_2)]^T$; $\beta = \text{diag}(\beta_1, \beta_2)$ and

$$\begin{aligned}\mathbf{h} = {} & C_1\left(K_1[u \quad v]^T + K_2[\theta \quad \phi]^T - \dot{\mathbf{y}}_r\right) + C_2\Big(K_1^2[u \quad v]^T + K_1K_2[\theta \quad \phi]^T \\ & + K_2[q \quad p]^T - \ddot{\mathbf{y}}_r\Big) + K_1^3[u \quad v]^T + K_1^2K_2[\theta \quad \phi]^T + K_1K_2[q \quad p]^T \\ & + K_2K_4[u \quad v \quad q \quad p]^T - \dddot{\mathbf{y}}_r.\end{aligned} \tag{46}$$

4.2.3. Stability analysis

Theorem 2 *Suppose system (17) satisfy assumptions 4 and 7 then system (17) under the proposed control law (45) is asymptotically stable if the high frequency switching gain in the control law is designed such that the following two conditions hold*

$$\beta_1 > |([1 \quad 0]\ M^*)| \tag{47}$$

and

$$\beta_2 > |([0 \quad 1]\ M^*)|, \tag{48}$$

where

$$\begin{aligned}M^* = {} & -\left[C_1 + K_1^2 + C_2K_1 + l_1(C_2 + K_1) + l_2(I_{2\times 2})\right]\mathbf{e}^*_{d1} \\ & -[C_2K_2 + K_1K_2 + l_2K_2]\mathbf{e}^*_{d2} - K_2\mathbf{e}^*_{d3};\end{aligned}$$

$$\mathbf{e}^*_{d1} = \left[e^*_{dt1} \quad e^*_{dt2}\right]^T; \quad \mathbf{e}^*_{d2} = \left[e^*_{dt3} \quad e^*_{dt4}\right]^T \quad \textit{and} \quad \mathbf{e}^*_{d3} = \left[e^*_{dt5} \quad e^*_{dt6}\right]^T.$$

Proof. Differentiating the sliding surface (42) gives

$$\begin{aligned}\dot{\mathbf{S}} = {} & \mathbf{h} + K_2K_3\mathbf{u}_{c1} + C_1\mathbf{d}_{tr1} + C_2(K_1\mathbf{d}_{tr1} + K_2\mathbf{d}_{tr2}) + K_1^2\mathbf{d}_{tr1} + K_1K_2\mathbf{d}_{tr2} \\ & + K_2\mathbf{d}_{tr3} + (K_1 + C_2)\dot{\mathbf{d}}_{tr1} + K_2\dot{\mathbf{d}}_{tr2} + \dddot{\mathbf{d}}_{tr1}.\end{aligned} \tag{49}$$

Expanding (25) gives

$$\dot{\mathbf{d}}_{tr2} = -l_1\mathbf{e}_{d1} + \hat{\dot{\mathbf{d}}}_{tr1}, \tag{50}$$

$$\dot{\mathbf{d}}_{tr2} = -l_1\mathbf{e}_{d2} + \hat{\mathbf{d}}_{tr2}, \tag{51}$$

where $\mathbf{e}_{d1} = [e_{dt1} \quad e_{dt2}]^T$ and $\mathbf{e}_{d2} = [e_{dt3} \quad e_{dt4}]^T$. Similarly (27) gives

$$\dddot{\mathbf{d}}_{tr1} = -l_2\mathbf{e}_{d1} + \hat{\dddot{\mathbf{d}}}_{tr1}. \tag{52}$$

Substituting (50), (51) and (52) in (49) gives

$$\begin{aligned}\dot{\mathbf{S}} &= \mathbf{h} + K_2K_3\mathbf{u}_{c1} + C_1\mathbf{d}_{tr1} + C_2\left(K_1\mathbf{d}_{tr1} + K_2\mathbf{d}_{tr2}\right)\\ &+ \left(C_2 + K_1\right)\left(-l_1\mathbf{e}_{d1} + \hat{\dot{\mathbf{d}}}_{tr1}\right) + K_2\left(-l_1\mathbf{e}_{d2} + \hat{\dot{\mathbf{d}}}_{tr2}\right)\\ &+ K_1^2\mathbf{d}_{tr1} + K_1K_2\mathbf{d}_{tr2} + K_2\mathbf{d}_{tr3} - l_2\mathbf{e}_{d1} + \hat{\ddot{\mathbf{d}}}_{tr1}.\end{aligned} \tag{53}$$

Substituting the control law (45) in (53) gives

$$\begin{aligned}\dot{\mathbf{S}} &= -\left[C_1 + K_1^2 + C_2K_1 + l_1\left(C_2 + K_1\right) + l_2\left(I_{2\times 2}\right)\right]\mathbf{e}_{d1}\\ &- \left[C_2K_2 + K_1K_2 + l_2K_2\right]\mathbf{e}_{d2} - K_2\mathbf{e}_{d3} - \beta\,\mathrm{sgn}(\mathbf{S})\\ &= M - \beta\,\mathrm{sgn}(\mathbf{S}),\end{aligned} \tag{54}$$

where M is bounded by M^*. Using the conditions (47) and (48) it is concluded from (54) that the system will reach the sliding surface $\mathbf{S} = \mathbf{0}$. At condition $\mathbf{S} = \mathbf{0}$, (42) becomes

$$\hat{\ddot{\mathbf{e}}}_y = -C_1\mathbf{e}_y - C_2\hat{\dot{\mathbf{e}}}_y. \tag{55}$$

Substituting (38) and (39) in (55) gives

$$\ddot{\mathbf{e}}_y = -\left[C_1\mathbf{e}_y + C_2\dot{\mathbf{e}}_y + \left(K_1 + C_2\right)\mathbf{e}_{d1} + K_2\mathbf{e}_{d2} + \mathbf{e}_{\dot{\mathbf{d}}\mathbf{1}}\right]. \tag{56}$$

Combining (56) with EDOB error dynamics (29) gives

$$\begin{aligned}\ddot{\mathbf{e}}_y &= -\left[C_1\mathbf{e}_y + C_2\dot{\mathbf{e}}_y + \left(K_1 + C_2\right)\mathbf{e}_{d1} + K_2\mathbf{e}_{d2} + \mathbf{e}_{\dot{\mathbf{d}}\mathbf{1}}\right],\\ \dot{\mathbf{e}}_{d1} &= -l_1\mathbf{e}_{d1} + \mathbf{e}_{\dot{\mathbf{d}}\mathbf{1}},\\ \dot{\mathbf{e}}_{d2} &= -l_1\mathbf{e}_{d2} + \mathbf{e}_{\dot{\mathbf{d}}\mathbf{2}},\\ \dot{\mathbf{e}}_{\dot{d}1} &= -l_2\mathbf{e}_{d1} + \mathbf{e}_{\ddot{\mathbf{d}}\mathbf{1}},\\ \dot{\mathbf{e}}_{\dot{d}2} &= -l_2\mathbf{e}_{d2} + \mathbf{e}_{\ddot{\mathbf{d}}\mathbf{2}},\\ \dot{\mathbf{e}}_{\ddot{d}1} &= -l_3\mathbf{e}_{d1} + \dddot{\mathbf{d}}_{tr1},\\ \dot{\mathbf{e}}_{\ddot{d}2} &= -l_3\mathbf{e}_{d2} + \dddot{\mathbf{d}}_{tr2}.\end{aligned} \tag{57}$$

Let

$$\begin{aligned}\boldsymbol{\varepsilon} &= \left[\boldsymbol{\varepsilon}_1 \quad \boldsymbol{\varepsilon}_2 \quad \boldsymbol{\varepsilon}_3 \quad \boldsymbol{\varepsilon}_4 \quad \boldsymbol{\varepsilon}_5 \quad \boldsymbol{\varepsilon}_6 \quad \boldsymbol{\varepsilon}_7 \quad \boldsymbol{\varepsilon}_8\right]\\ &= \left[\mathbf{e}_y \quad \dot{\mathbf{e}}_y \quad \mathbf{e}_{d1} \quad \mathbf{e}_{d2} \quad \mathbf{e}_{\dot{d}1} \quad \mathbf{e}_{\dot{d}2} \quad \mathbf{e}_{\ddot{d}1} \quad \mathbf{e}_{\ddot{d}2}\right]\end{aligned} \tag{58}$$

and

$$\dddot{\mathbf{d}}_{12} = \left[\dddot{\mathbf{d}}_{tr1} \quad \dddot{\mathbf{d}}_{tr1}\right]^T, \tag{59}$$

$$\|\dddot{\mathbf{d}}_{12}\| \leqslant \mu_{3r}, \tag{60}$$

where μ_{3r} is positive bounded constant. Then (57) is written in state space form as

$$\dot{\varepsilon} = A_\varepsilon \boldsymbol{\varepsilon} + B_\varepsilon \dddot{\mathbf{d}}_{12}, \tag{61}$$

where A_ε and B_ε are given as

$$A_\varepsilon = \left[\begin{array}{c|cccccc} & 0 & 0 & 0 & 0 & 0 & 0 \\ A_{\varepsilon r} & -(K_1+C_2) & -K_2 & -1 & 0 & 0 & 0 \\ -- & -- & -- & -- & -- & -- & -- \\ 0_{12\times 4} & & & D_r & & & \end{array}\right];$$
$$B_\varepsilon = \left[\begin{array}{cccc} 0_{4\times 4} & 0_{4\times 4} & 0_{4\times 4} & I_{4\times 4} \end{array}\right]^T \tag{62}$$

and

$$A_{\varepsilon r} = \left[\begin{array}{cc} 0 & 1 \\ -C_1 & -C_2 \end{array}\right]; \qquad D_r = \left[\begin{array}{ccc} -l_1 I_{4\times 4} & I_{4\times 4} & 0_{4\times 4} \\ -l_2 I_{4\times 4} & 0_{4\times 4} & I_{4\times 4} \\ -l_3 I_{4\times 4} & 0_{4\times 4} & 0_{4\times 4}]] \end{array}\right] \tag{63}$$

as A_ε is block triangular matrix, its eigenvalues are given by the following equation

$$\det(\lambda I_{4\times 4} - A_{\varepsilon 1}) \cdot \det(\lambda I_{12\times 12} - D_r) = 0 \tag{64}$$

where $\det(\cdot)$ denotes the determinant of a matrix and $\lambda \in R$ is an eigenvalue of A_ε. Earlier (31) and (42) were designed Hurwitz so both $A_{\varepsilon r}$ and D_r are Hurwitz and all eigenvalues of A_ε have strictly negative real parts. As A_ε is Hurwitz so a positive definite matrix P_2 always exist satisfying the following equation

$$A_\varepsilon^T P_2 + P_2 A_\varepsilon = -\mathrm{Q}_2 . \tag{65}$$

Defining the following Lyapunov function

$$V(\boldsymbol{\varepsilon}) = \boldsymbol{\varepsilon}^T P_2 \boldsymbol{\varepsilon}. \tag{66}$$

Differentiating $V(\boldsymbol{\varepsilon})$ with respect to time t gives

$$\begin{aligned} \dot{V}(\boldsymbol{\varepsilon}) &= \boldsymbol{\varepsilon}^T \left(A_\varepsilon^T P_2 + P_2 A_\varepsilon\right) \boldsymbol{\varepsilon} + 2\boldsymbol{\varepsilon}^T P_2 B_\varepsilon \dddot{\mathbf{d}}_{12} \\ &\leqslant -\boldsymbol{\varepsilon}^T (\mathrm{Q}_2)\, \boldsymbol{\varepsilon} + 2\mathbf{e}^T \lambda_{\max}(P_2)\, \mu_{3r} \\ &\leqslant -\|\boldsymbol{\varepsilon}\| \left[\lambda_{\min}(\mathrm{Q}_2) \|\boldsymbol{\varepsilon}\| - 2\lambda_{\max}(P_2)\, \mu_{3r}\right]. \end{aligned} \tag{67}$$

From $\dot{V}(\boldsymbol{\varepsilon}) \leqslant 0$, it is concluded that the states of the system (61) converges asymptotically inside a ball $b_1 \in R^{16}$ and stay inside for the remaining period of time such that

$$\|\boldsymbol{\varepsilon}\| \leqslant 2\mu_{3r}\left[\lambda_{\max}(P_2)/\lambda_{\min}(\mathrm{Q}_2)\right]. \tag{68}$$

□

5. Heading-heave subsystem

In this section, ST-SMC method is used to derive the control laws u_{ped} and u_{col} for heading and vertical velocity tracking of the helicopter in presence of external disturbances. The subsystem (7) is divided in two separate systems as

$$\begin{aligned} \dot{\psi} &= r, \\ \dot{r} &= N_v v + N_w w + N_r r + N_{ped} u_{ped} + N_{col} u_{col} + d_{t7}, \\ y_{21} &= \psi; \end{aligned} \tag{69}$$

$$\begin{aligned} l\dot{w} &= Z_w w + Z_{col} u_{col} + d_{t8}, \\ y_{22} &= w, \end{aligned} \tag{70}$$

where (69) and (70) represent the heading dynamics and the heave dynamics of the helicopter respectively, N_v, N_w, N_r and Z_w are stability derivatives, N_{ped}, N_{col} and Z_{col} are input derivatives, d_{t7} and d_{t8} are the total disturbances (including model mismatch and external disturbances). Both d_{t7} and d_{t8} are matched disturbances (acting at control input channel) and there is no need of disturbance observer for (69) and (70) as SMC is insensitive to matched disturbance.

5.1. Controller for heading dynamics

The yaw tracking error e_ψ and its derivative are defined as

$$e_\psi = \psi - \psi_r, \tag{71}$$

$$\dot{e}_\psi = r - \dot{\psi}_r. \tag{72}$$

The sliding surface for controller design is defined as

$$S_\psi = c_\psi e_\psi + \dot{e}_\psi, \tag{73}$$

where $c_\psi > 0$ so that $S_\psi = 0$ is Hurwitz. Then the ST-SMC law is designed as

$$\begin{aligned} u_{ped} = -1/N_{ped} \Big(& c_\psi \dot{e}_\psi - \dot{\psi}_r + N_v v + N_w w + N_r r + N_{col} u_{col} \\ & + k_{\psi 1} \left| s_\psi \right|^{1/2} \operatorname{sgn}\left(s_\psi\right) + k_{\psi 2} \int \operatorname{sgn}(s_\psi) \, \mathrm{d}\, s_\psi \Big). \end{aligned} \tag{74}$$

Theorem 3 *System (69) under the proposed control law (74) is ultimately exponentially stable if the following condition holds*

$$k_{\psi 2} > \mu_{71}, \tag{75}$$

where μ_{71} is positive bounded constant such that $\dot{d}_{t7} < \mu_{71}$.

Proof. Differentiating the sliding surface (73) gives

$$\dot{s}_\psi = c_\psi \dot{e}_\psi + N_v v + N_w w + N_r r + N_{ped} u_{ped} + N_{col} u_{col} - \dot{\psi}_r + \dot{d}_{t7} \,. \tag{76}$$

Substituting the control law (74) in (76) gives

$$\dot{s}_\psi = -k_{\psi 1} \left| s_\psi \right|^{1/2} \operatorname{sgn}\left(s_\psi\right) - k_{\psi 2} \int \operatorname{sgn}(s_\psi) \, \mathrm{d}\, s_\psi + \dot{d}_{t7} \,. \tag{77}$$

Dynamics of (77) is similar to a usual super twisting algorithm and from [29] it is known that (77) is finite time stable and S_ψ and $\dot{S}_\psi$ will converge to zero in finite time. At condition $S_\psi = 0$, (73) becomes

$$\dot{e}_\psi = -c_\psi e_\psi \,. \tag{78}$$

As (78) is exponentially stable so it is concluded that the yaw tracking error e_ψ will ultimately exponentially converge to zero. □

5.2. Controller for heave dynamics

The vertical velocity tracking error e_ψ is defined as

$$e_w = w - w_r \,. \tag{79}$$

Then the ST-SMC law is designed as

$$u_{col} = -1/Z_{col} \Big(- \dot{w}_r + Z_w w + k_{w1} \left| e_w \right|^{1/2} \operatorname{sgn}\left(e_w\right) + k_{w2} \int \operatorname{sgn}(s_w) \, \mathrm{d}\, s_w \Big). \tag{80}$$

Theorem 4 *System (70) under the proposed control law (80) is finite time stable if the following condition holds*

$$k_{w2} > \mu_{81}, \tag{81}$$

where μ_{81} *is positive bounded constant such that* $\dot{d}_{t8} < \mu_{81}$.

Proof. Differentiating (79) and substituting (80) gives

$$\dot{e}_w = -k_{w1} \left| e_w \right|^{1/2} \operatorname{sgn}\left(e_w\right) - k_{w2} \int \operatorname{sgn}(s_w) \, \mathrm{d}\, s_w + \dot{d}_{t8} \,. \tag{82}$$

Dynamics of (82) is similar to a usual super twisting algorithm and from [29] it is known that (82) is finite time stable and the tracking error e_w and its derivative $\dot{e}_w$ will converge to zero in finite time. □

6. Simulation results

In this section performance of the proposed EDOB-SMC (45) is evaluated. Two numerical simulations are presented, the first simulation is performed in absence of external disturbance while the second simulation is performed in presence of external disturbances. To show the effectiveness of the proposed EDOB-SMC (45), an integral sliding mode controller (ISMC) is used in these simulations for performance comparison. The sliding surface of the ISMC method is designed as

$$\begin{aligned}\boldsymbol{\sigma} = &(\ddot{\mathbf{y}}_1 - \ddot{\mathbf{y}}_r) + C_3(\dot{\mathbf{y}}_1 - \dot{\mathbf{y}}_r) + C_2(\mathbf{y}_1 - \mathbf{y}_r) + C_1 \int (\mathbf{y}_1 - \mathbf{y}_r) \\ &- (C_3 + K_1)\,\mathbf{d}_{tr1} - K_2\mathbf{d}_{tr2} - \dot{\mathbf{d}}_{tr1}\,.\end{aligned} \tag{83}$$

Substituting $\dot{\mathbf{y}}_1$ and $\ddot{\mathbf{y}}_1$ in (47) the disturbance terms $(-(C_3 + K_1)\mathbf{d}_{tr1} - K_2\mathbf{d}_{tr2} - \dot{\mathbf{d}}_{tr1})$ get cancelled. So its a typical sliding surface for I-SMC. Then the I-SMC is designed as

$$\mathbf{u}_{c1} = (-K_2K_3)^{-1}\left(\mathbf{h}_i + \beta_i \operatorname{sgn}(\boldsymbol{\sigma})\right), \tag{84}$$

where

$$\begin{aligned}\mathbf{h}_i = &C_1(\mathbf{y}_1 - \mathbf{y}_r) + C_2\left(K_1[u \quad v]^T + K_2[\theta \quad \phi]^T - \dot{\mathbf{y}}_r\right) \\ &+ C_3\left(K_1^2[u \quad v]^T + K_1K_2[\theta \quad \phi]^T + K_2[q \quad p]^T - \ddot{\mathbf{y}}_r\right) \\ &+ K_1^3[u \quad v]^T - \dddot{\mathbf{y}}_r + K_1K_2[q \quad p]^T \\ &+ K_2K_4[u \quad v \quad q \quad p]^T + K_1^2K_2[\theta \quad \phi]^T,\end{aligned} \tag{85}$$

$$\beta_i \operatorname{sgn}(\boldsymbol{\sigma}) = \operatorname{diag}\left(\beta_3 \operatorname{sgn}(\sigma_1),\ \beta_4 \operatorname{sgn}(\sigma_2)\right) \tag{86}$$

and

$$\beta_3 > \max_{t>0}\left|[1 \quad 0]\left(-(C_3 + K_1)\mathbf{d}_{tr1} - K_2\mathbf{d}_{tr2} - \dot{\mathbf{d}}_{tr1}\right)\right|, \tag{87}$$

$$\beta_4 > \max_{t>0}\left|[0 \quad 1]\left(-(C_3 + K_1)\mathbf{d}_{tr1} - K_2\mathbf{d}_{tr2} - \dot{\mathbf{d}}_{tr1}\right)\right|. \tag{88}$$

Raptor 90 SE radio controlled helicopter is used in these simulation. The Simulink model is established using the nonlinear model of the helicopter defined in (1) and then the proposed EDOB-SMC (45), ST-SMC (74), (80) and the I-SMC (84), ST-SMC (74), (80) based on the reduced order linearized model (17) are applied on it for performance evaluation. Parameters of the nonlinear model of the helicopter are given in Table 1 and parameters of the reduced order linearized model are given in Table 2.

Table 1: Parameters of Raptor 90SE RC helicopter [30]

Nonlinear model parameters		
m = 7.495 kg	Ω = 172.788 rad/s	R = 0.785 m
$b_m = 2$	c_m = 0.060 m	ρ = 1.290 kg/m^3
g = 9.81 m/s^2	$C_{l\alpha}^m = 4.0734$	$k_a = 9.4248$
$k_{col} = 0.3813$	k_β = 167.6592 N.m/rad	$h_{mr} = 0.275$ m
I_{xx} = 0.1895 kgm^2	I_{yy} = 0.4515 kg m^2	I_{zz} = 0.3408 kg m^2
$N_v = 2.982$	$N_p = 0$	$N_w = -0.7076$
$N_r = -10.71$	$N_{ped} = 26.90$	$N_{col} = 3.749$
t_f = 0.03256 sec	$A_b = 0.7713$	$B_a = 0.6168$
$A_{lon} = 4.059$	$A_{lat} = -0.01610$	$B_{lon} = -0.01017$
$B_{lat} = 4.085$		

Table 2: Parameters of the linearized model [11]

Parameters of A_{11}, A_{21} and A_{22}		
$X_u = -0.03996$	$Y_v = -0.05989$	$1/t_f = 30.71$
$M_u = 0.2542$	$M_v = -0.06013$	$Z_w = -2.055$
$L_u = -0.0244$	$L_v = -0.1173$	$N_v = 2.982$
$M_a = 307.571$	$L_b = 1172.4817$	$N_r = -10.71$
$A_b = 0.7713$	$B_a = 0.6168$	$N_w = -0.7076$
Parameters of B_{11} and B_{22}		
$A_{lon} = 4.059$	$A_{lat} = -0.01610$	$B_{lat} = 4.085$
$B_{lon} = -0.01017$	$Z_{col} = -13.11$	$N_{col} = 3.749$
$N_{ped} = 26.90$		
Parameters of A_r and B_r		
$M_q = 10.0153$	$M_p = 0.2515$	$L_p = 38.1792$
$L_q = 0.7667$	$M_{lon} = 40.6609$	$M_{lat} = 0.8662$
$L_{lon} = 2.7238$	$L_{lat} = 155.9401$	

The reference velocity vector $\mathbf{v}_r^B = [u_r \;\; v_r \;\; w_r]^T$ in the body frame is obtained as

$$\mathbf{v}_r^B = R^T \mathbf{v}_r^I, \tag{89}$$

where R^T is the rotation matrix representing the orientation of the inertial frame in body fixed frame of the helicopter. The reference velocity trajectories $\mathbf{v}_r^I$ for the whole flight are produced by a low pass filter $1/(s+2)^3$ with input $\mathbf{V}_r^I$ given as

$$\mathbf{V}_r^I = V_{\max} \begin{cases} [0 \;\; 0 \;\; 0]^T & \text{for } t < 0.5, \\ \begin{bmatrix} 0 \\ 0 \\ -2\sin\left(\frac{\pi}{7}(t-0.5)\right) \end{bmatrix} & \text{for } 0.5 \leqslant t < 7, \\ [0 \;\; 0 \;\; 0]^T & \text{for } 7.5 \leqslant t < 12.5, \\ \begin{bmatrix} 10\sin\left(\frac{\pi}{32}(t-12.5)\right) \\ 3\sin\left(\frac{\pi}{32}(t-12.5)\right) \\ 0 \end{bmatrix} & \text{for } 12.5 \leqslant t < 28.5, \\ [10 \;\; 3 \;\; 0]^T & \text{for } 28.5 \leqslant t < 40, \\ \begin{bmatrix} 10\cos\left(\frac{\pi}{40}(t-40)\right) \\ 3\cos\left(\frac{\pi}{40}(t-40)\right) \\ 0 \end{bmatrix} & \text{for } 40 \leqslant t < 60, \\ [0 \;\; 0 \;\; 0]^T & \text{for } t \geqslant 60, \end{cases} \tag{90}$$

where $V_{\max} = \operatorname{diag}(v_{\max 1}, \; v_{\max 2}, \; v_{\max 3})$ is tuning gain matrix to ensure $\max(u_r) = 10$, $\max(v_r) = 3$ and $\max(w_r) = 2$. Throughout all the flight the reference heading angle is constant with a value of $\psi_r = 0$.

6.1. Trajectory tracking in absence of external disturbances

In first case performance comparison of the two controllers EDOB-SMC (45), ST-SMC (74), (80) and the I-SMC (84), ST-SMC (74), (80) is done in absence of external disturbances. The reference fight path to be tracked is given in (89). All initial states of the helicopter system (1) are set as zero except $\psi = 0.001$ rad.

Parameters of the EDOB-SMC are $C_1 = \text{diag}(10, 10)$; $C_2 = \text{diag}(25, 25)$; $\beta_1 = 2.5$; $\beta_2 = 2.5$; $l_1 = 18$; $l_2 = 108$; $l_3 = 216$ while parameters of the I-SMC are $C_1 = \text{diag}(125, 125)$; $C_2 = \text{diag}(75, 75)$; $C_3 = \text{diag}(15, 15)$; $\beta_1 = 2.5$; $\beta_2 = 2.5$. Parameters of u_{ped} and u_{col} are $c_\psi = 5$; $k_{\psi 1} = 2$; $k_{\psi 2} = 3$; $k_{w1} = 1.3$; $k_{w2} = 5.5$. These parameters are tuned to get the best results. The switching gains of EDOB-SMC are tuned by gradually increasing it from zero until no significant improvement is observed in tracking performance and the same gains are used for ISMC. The simulation results in case 1 are given in Figs. 2–7. Fig. 2 shows the results of velocity tracking and Fig. 3 shows the response curves of Euler angles. The velocity and yaw tracking error are given in Fig. 4. The disturbances in the log-lat subsystem, estimated by EDOB are given in Fig. 5, as no external disturbances were applied so its a measure of the total model mismatch present in log-lat subsystem during the flight. It is clear that EDOB-SMC has higher accuracy and better tracking performance. In case of ISMC, the closed loop system is stable but the tracking error is very high compared to EDOB-SMC. Figs. 6 and 7 show the control inputs and the chattering are within reasonable range.

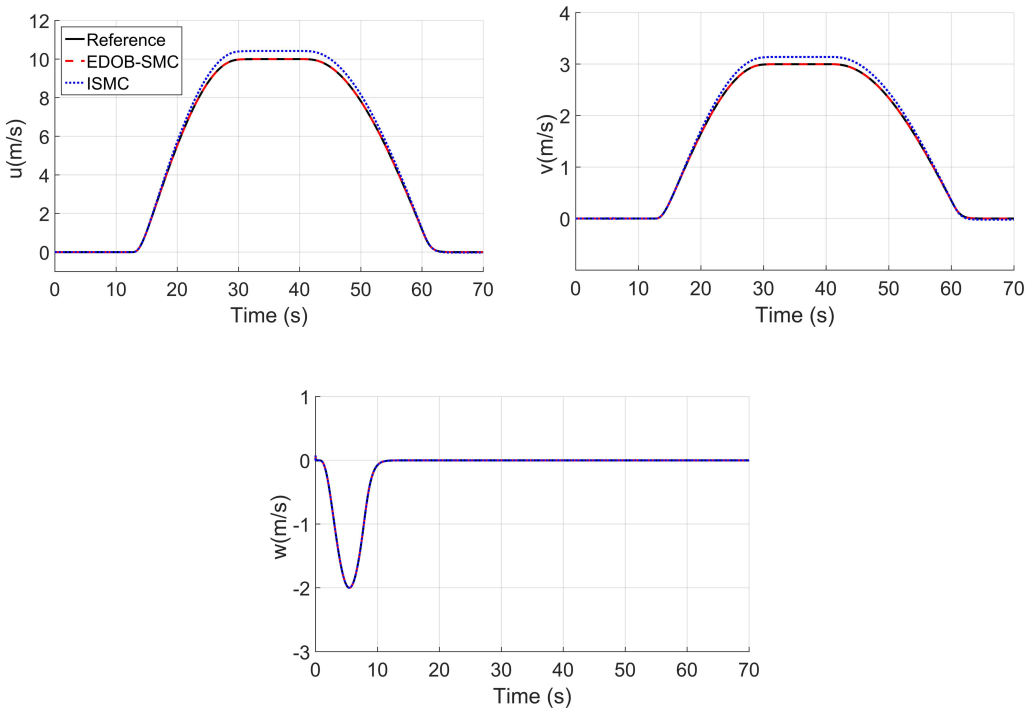

Figure 2: Velocity tracking responses expressed in body coordinate system

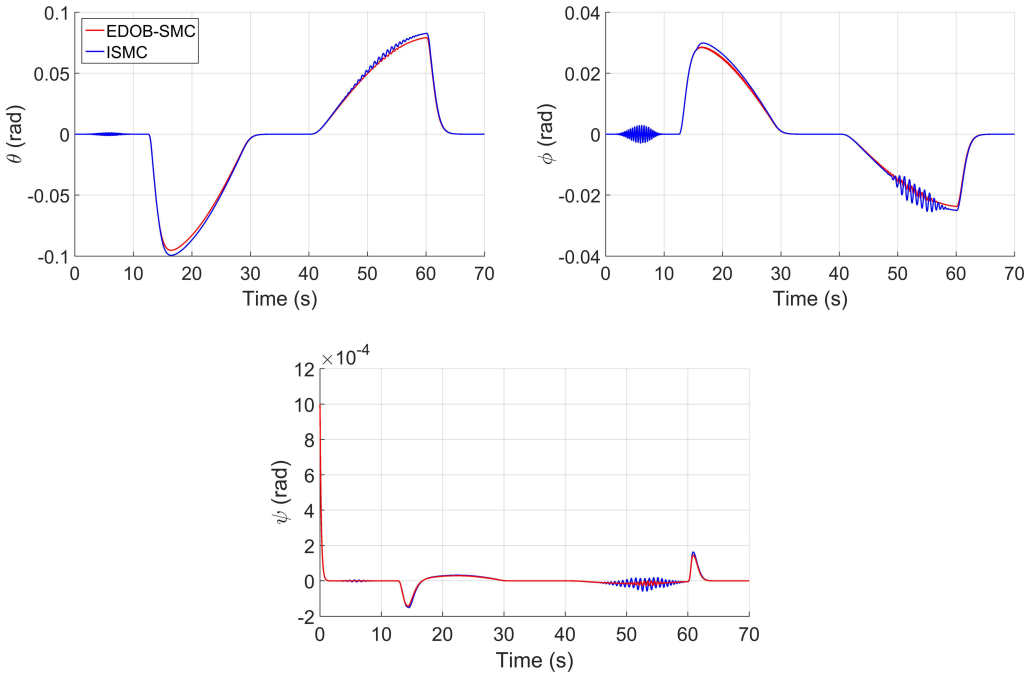

Figure 3: Response curves of orientation angles

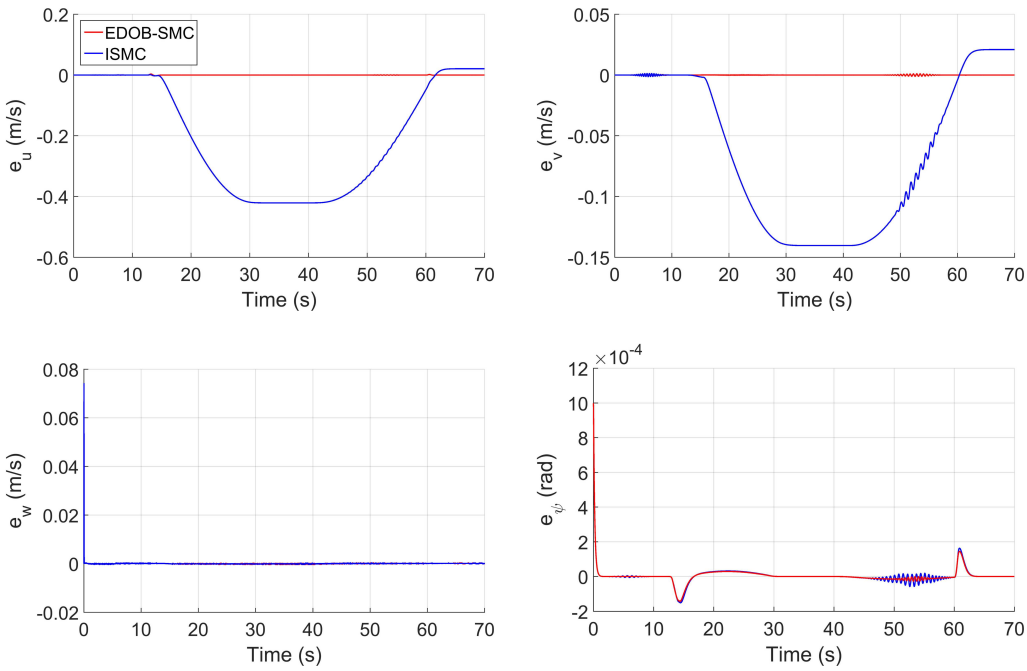

Figure 4: Response curves of tracking error

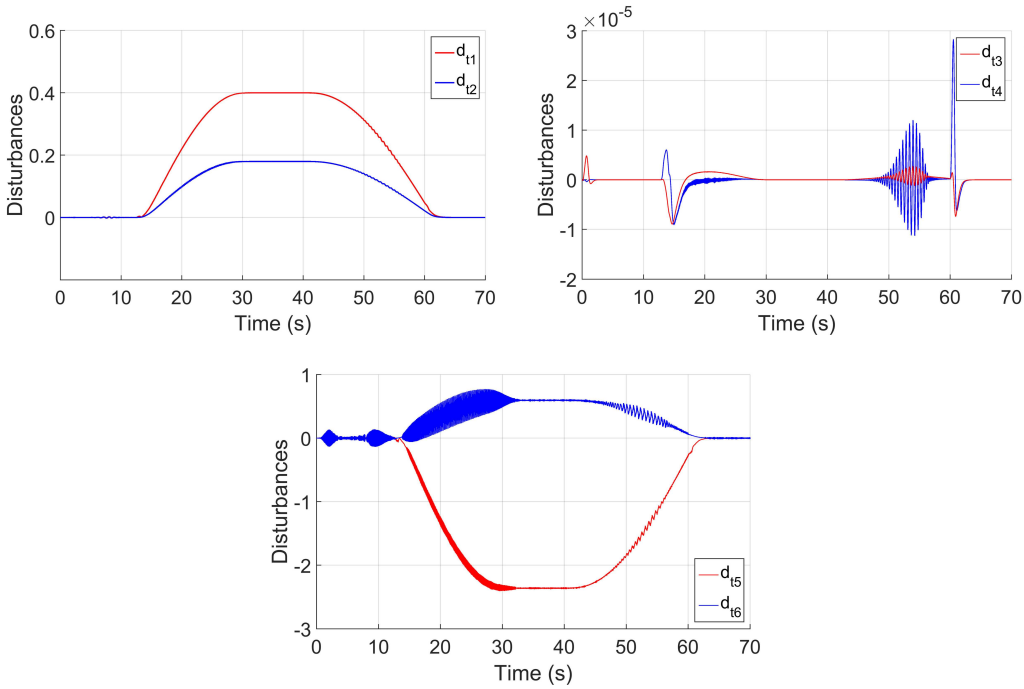

Figure 5: Disturbances approximated by EDOB

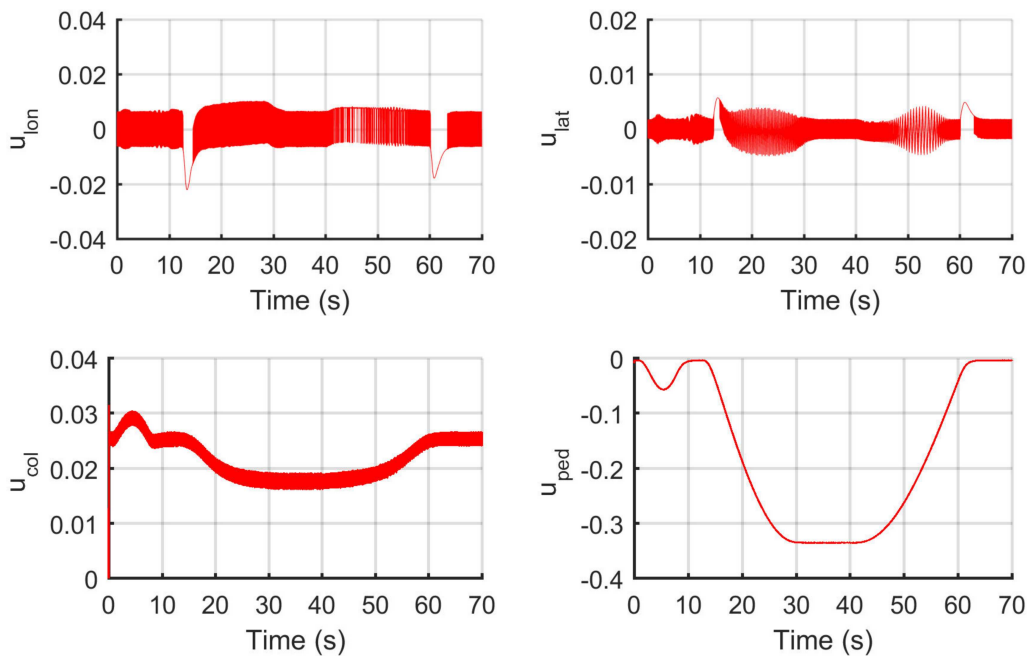

Figure 6: Control inputs of EDOB-SMC

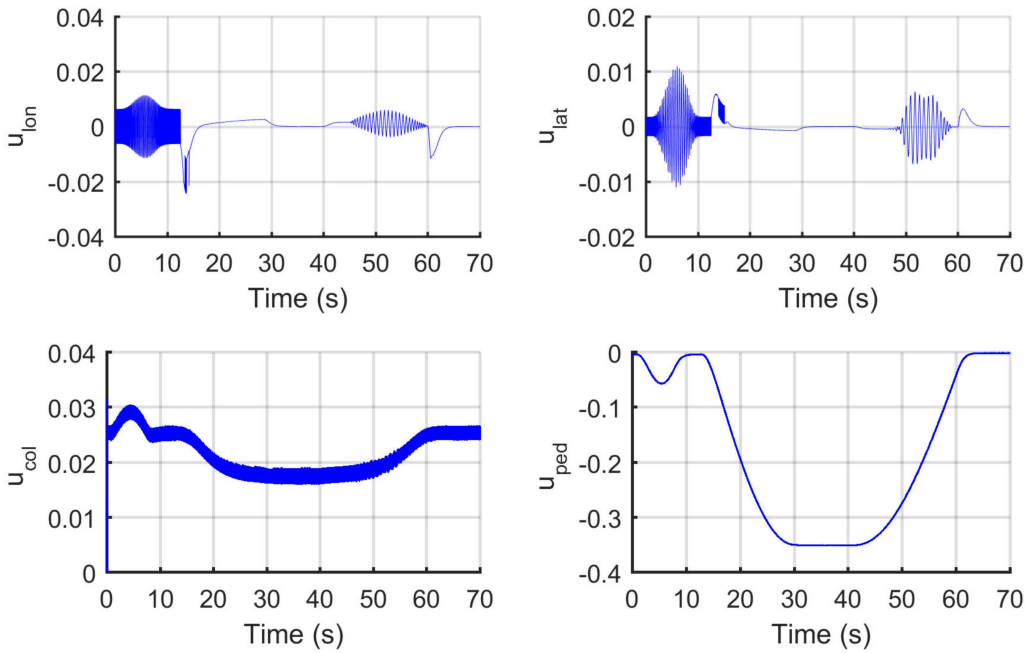

Figure 7: Control inputs of ISMC

6.2. Trajectory tracking in presence of external disturbances

In the second case performance comparison of the two controllers EDOB-SMC (45), ST-SMC (74), (80) and the I-SMC (84), ST-SMC (74), (80) is done in presence of external wind disturbances $\left(\mathbf{D}_w^B = [d_{w1} \quad d_{w2} \quad d_{w3}]^T\right)$ acting on the helicopter are given as

$$\mathbf{D_w^B} = \begin{cases} [0;\ 0;\ 0]^T & \text{for } t < 13, \\ \begin{bmatrix} -0.3\sin\left(\frac{\pi}{2}(t-1)\right) \\ -0.2\sin\left(\frac{\pi}{2}(t-1)\right) \\ 0 \end{bmatrix} & \text{for } 13 \leqslant t < 33, \\ \left[0;\ 0;\ 0.2\sin\left(\frac{\pi}{2}(t-1)\right)\right]^T & \text{for } 33 \leqslant t < 45, \\ [0;\ 0;\ 0]^T & \text{for } t \geqslant 45. \end{cases} \tag{91}$$

The reference fight path to be tracked, all initial states of the helicopter system (1) and parameters of the controllers are same as in case1. The simulation results in case 2 are given in Figs. 8–13. Fig. 8 shows results of the velocity tracking and

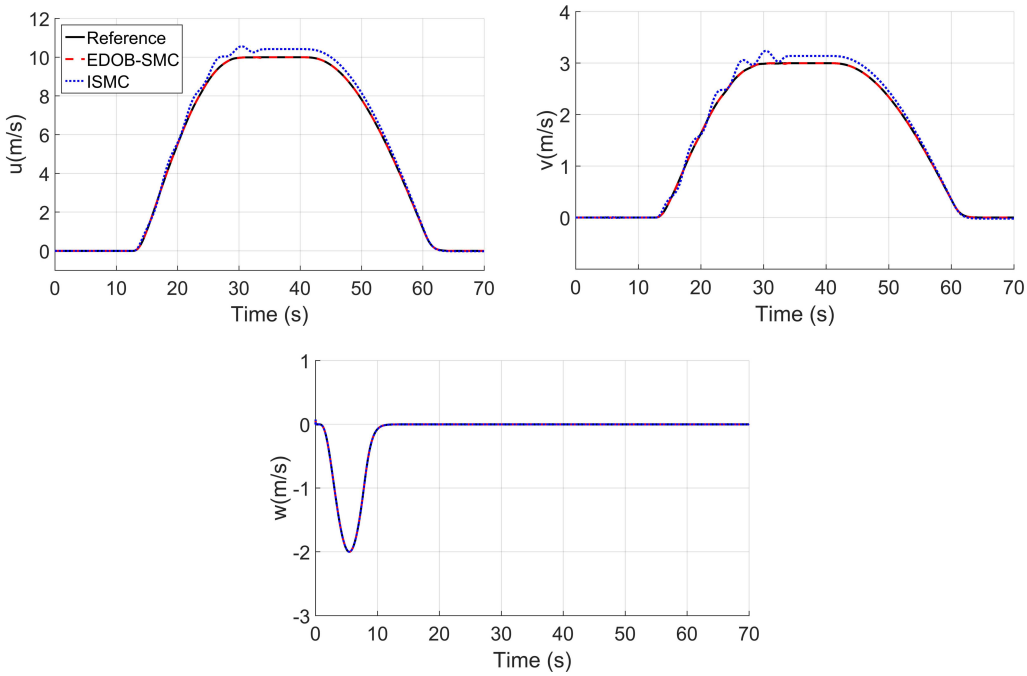

Figure 8: Velocity tracking responses expressed in body coordinate system

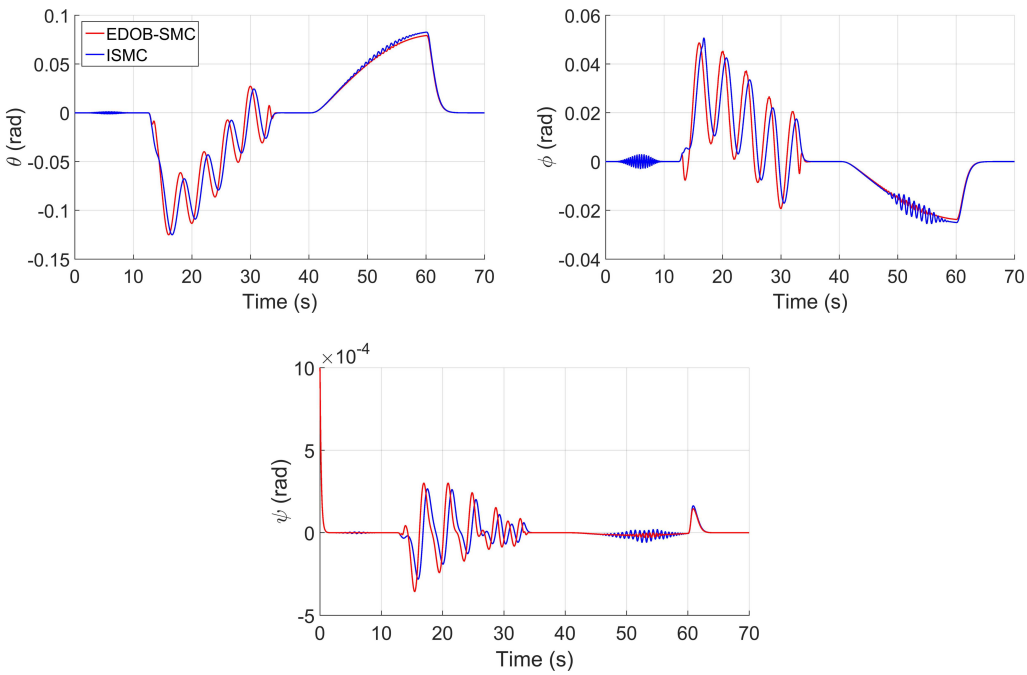

Figure 9: Response curves of orientation angles

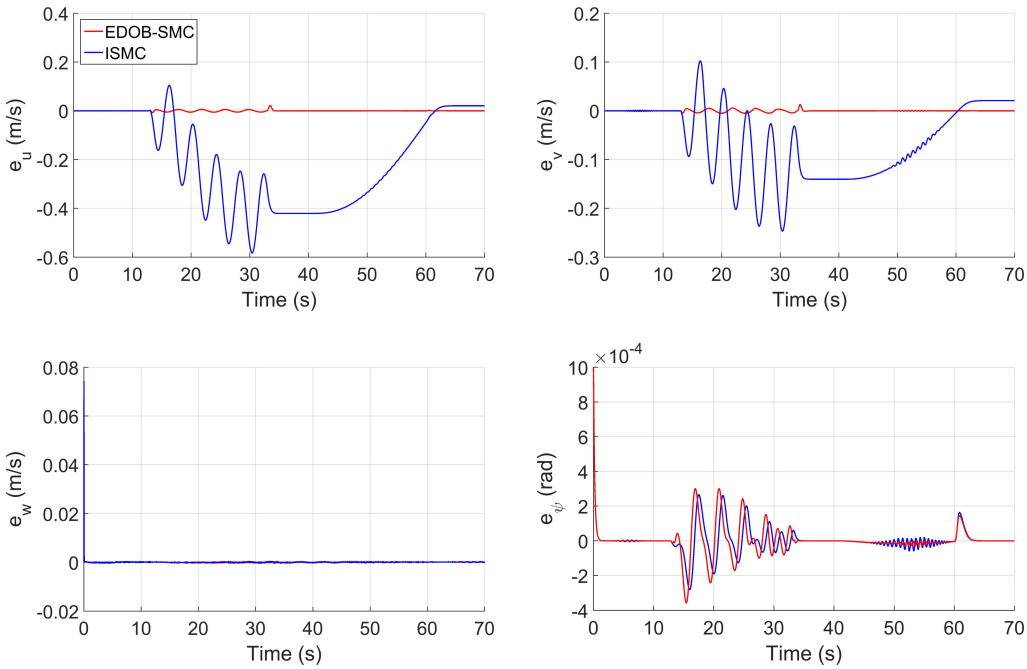

Figure 10: Response curves of tracking error

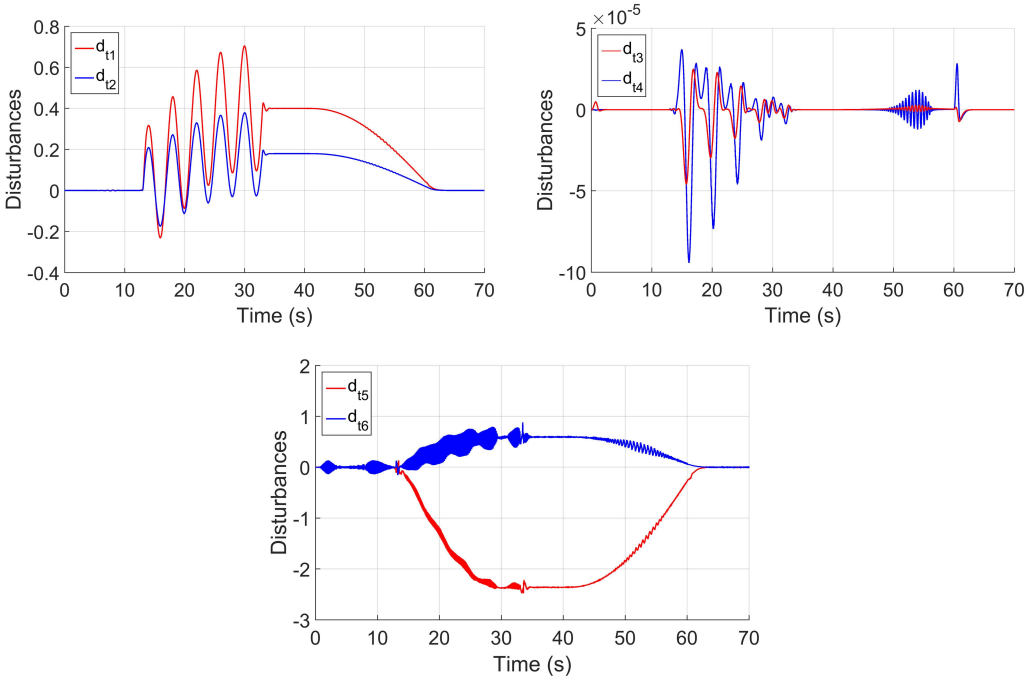

Figure 11: Disturbances approximated by EDOB

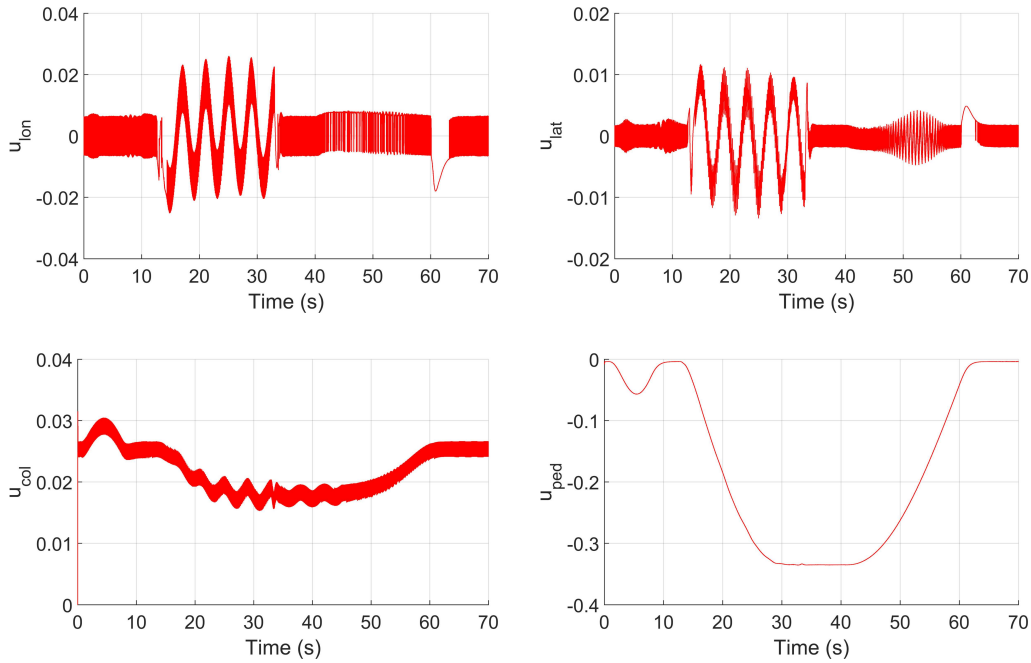

Figure 12: Control inputs of EDOB-SMC

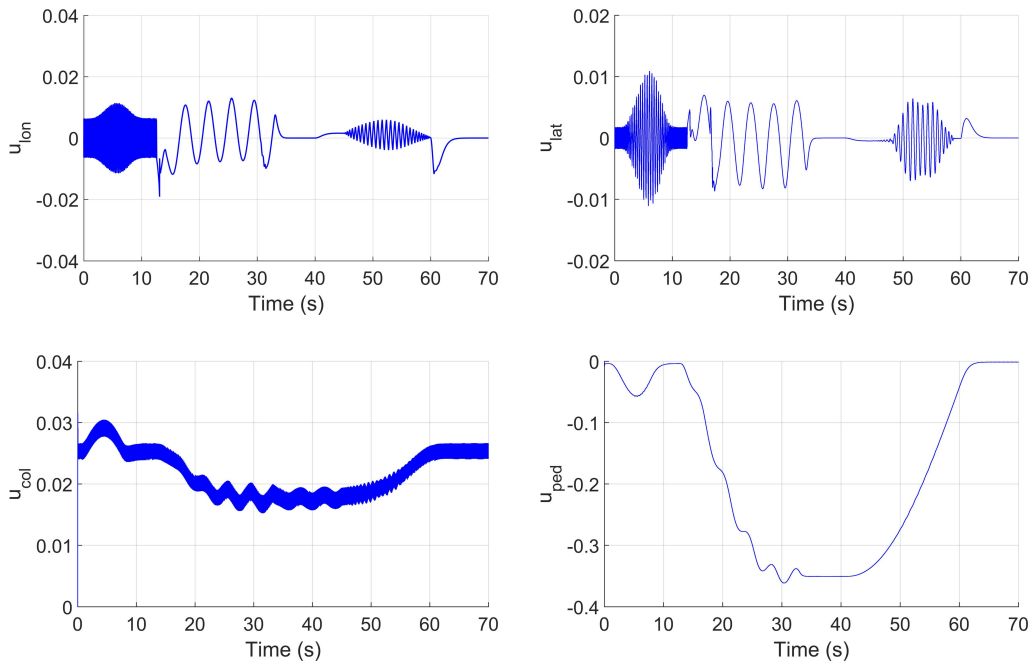

Figure 13: Control inputs of ISMC

Fig. 9 shows response curves of the Euler angles. The velocity and yaw tracking error are given in Fig. 10. The disturbances estimated by EDOB are given in Fig. 11 and it is a measure of the total model mismatch and external disturbances acting on log-lat subsystem during the flight. It is clear that EDOB-SMC has better capabilities to handle model mismatch and external disturbances and EDOB-SMC has higher accuracy and better tracking performance than ISMC. Figs. 12 and 13 shows the control inputs chattering are within reasonable range.

7. Conclusion

This paper presents a robust control technique for small-scale unmanned helicopters to track predefined velocities and heading trajectories in the presence of bounded external disturbances by taking advantage of the decoupled dynamics (longitudinal-lateral and heading-heave) of the helicopter. Separate controllers are designed for the longitudinal-lateral and heading-heave subsystem of the helicopter. The external disturbances and model mismatch in the longitudinal-lateral subsystem are estimated as lumped disturbances using EDOB. EDOB-SMC is designed for the longitudinal-lateral subsystem to counter the effect of these disturbances while a Second order sliding mode controller is designed for the heading-heave subsystem. The closed-loop asymptotic stability of the system is proved using the Lyapunov stability analysis and finally, the effectiveness of the proposed controller is shown by simulation results.

References

[1] J.G. Leishman: *Principles of Helicopter Aerodynamics*. Cambridge University Press 2006.

[2] H. Shim, T. Koo, and F. Hoffmann: A comprehensive study of control design for an autonomous helicopter. *Proceedings of the 37th IEEE Conference on Decision and Control* (1998), 3653–3658.

[3] E.N. Sanchez, H.M. Becerra, and C.M. Velez: Combining fuzzy pid and regulation control for an autonomous minihelicopter. *Information Sciences*, **177** (2007), 1999–2022.

[4] E. Lee, H. Shim, and H. Park: Design of hovering attitude controller for a model helicopter. *Proceedings of Society of Instrument and Control Engineers*, Tokyo (1993), 1385–1389.

[5] B. Guerreiro, C. Silvestre, and R. Cunha: Trajectory tracking H2 controller for autonomous helicopters. An application to industrial chimney inspection. *17th IFAC Symposium on Automatic Control in Aerospace*, Toulouse, France (2007), 431–436.

[6] I.B. Tijani, R. Akmeliawati, and A. Legowo: H∞ robust controller for autonomous helicopter hovering control. *Aircraft Engineering & Aerospace Technology*, **83** (2011), 363–374.

[7] L. Mollov, J. Kralev, T. Slavov, and P. Petkov: μ-synthesis and hardware-in-the-loop simulation of miniature helicopter control system. Journal of Intelligent & Robotic Systems, **76** (2014), 315-351.

[8] M.L. Civita, T. Kanade, W. Messner, and G. Papageorgiou: Design and flight testing of an H∞ controller for a robotic helicopter. *Journal of Guidance Control & Dynamics*, **29** (2006), 485–494.

[9] M.F. Weilenmann and H.P. Geering: A test bench for rotorcraft hover control. *AIAA Guidance, Navigation and Control Conference*, California USA (1993) 1371–1382.

[10] M.F. Weilenmann, U. Christen, and H.P. Geering: Robust helicopter position control at hover. *American Control Conference*, Maryland USA (1999), 2491–2495.

[11] I.A. Raptis, K.P. Valavanis, and G.J. Vachtsevanos: Linear tracking control for small-scale unmanned helicopters. *IEEE Transation on Control System Technology*, **20** (2012), 995–1010.

[12] C. Fan, S. Guo, and D. Li: Nonlinear predictive attitude control with a disturbance observer of an unmanned helicopter on the test bench. *IEEE 5th International Conference on Robotics, Automation and Mechatronics*, Qingdao China (2011), 304–309.

[13] D.C. Robinaon, K. Ryan, and H. Chung: Helicopter hovering attitude control using a direct feedthrough Simultaneous state and disturbance Observer. *IEEE Conference on Control Applications*, Sydney Australia (2015), 633–638.

[14] V.I. Utkin: *Sliding Mode in Control and Optimization*. Springer, 1992.

[15] H. Liu and S. Li: Speed control for PMSM servo system using predictive functional control and extended state observer. *IEEE Transaction of Industrial Electronics*, **59** (2012), 1171–1183.

[16] D. Chwa, J.Y. Choi, and J.H. Seo: Compensation of actuator dynamics in nonlinear missile control. *IEEE Transactions of Control System Technology*, **12** (2004), 620–626.

[17] W.H. Chen: Nonlinear disturbance observer-enhanced dynamic inversion control of missiles. *Journal of Guidance Control & Dynamics*, **26** (2003), 161–166.

[18] Y. He, H. Pei, and T. Sun: Robust tracking control of helicopters using backstepping with disturbance observers. *Asian Journal of Control*, **16** (2014), 1–16.

[19] Y.W. Liang, L.W. Ting, and L.G. Lin: Study of reliable control via an integral-type sliding mode control scheme. *IEEE Transaction of Industrial Electronics*, **59** (2012), 3062–3068.

[20] Q. Hu, L. Xie, Y. Wang, and C. Du: Robust tracking-following control of hard disk drives using improved integral sliding mode combined with phase lead peak filter. *International Journal of Adaptive Control & Signal Processing*, **22** (2008) 413–430.

[21] W.J. Cao and J.X. Xu: Nonlinear integral-type sliding surface for both matched and unmatched uncertain systems. *IEEE Transactions of Automatic Control*, **49** (2004), 1355–1360.

[22] J. Yang, S. Li, and X. Yu: Sliding-mode control for systems with mismatched uncertainties via a disturbance observer. *IEEE Transactions on Industrial Electronics*, **60** (2013), 160–169.

[23] D. Ginoya, P.D. Shendge, and S.B. Phadke: Sliding Mode Control for Mismatched Uncertain Systems Using an Extended Disturbance Observer. *IEEE Transactions on Industrial Electronics*, **61** (2014), 1983–1992.

[24] I. Ullah and H. Pei: Disturbance observer based sliding mode control for unmanned helicopter hovering operations in presence of external disturbances. *Incas Bulletin*, **10** (2018), 103–118.

[25] A. Budiyono and S.S. Wibowo: Optimal tracking controller design for a small scale helicopter. *Journal of Bionic Engineering*, **4** (2007), 272–279

[26] V. Gavrilets: *Dynamic model for a miniature aerobatic helicopter. Handbook of Unmanned Aerial Vehicles*. Springer, (2015) 279-306.

[27] S. Tang, L. Zhang, and S.K. Qian: Second-order sliding mode attitude controller design of a small-scale helicopter. *Science China Information Sciences*, **59** (2016), 112209–112214.

[28] C. Liu, W.H. Chen, and J. Andrews: Tracking control of small-scale helicopters using explicit nonlinear MPC augmented with disturbance observers. *Control Engineering Practice*, **20** (2012), 20258–268.

[29] A. Levant: Universal Single-Input-Single-Output (SISO) Sliding- Mode Controllers with Finite-Time Convergence. IEEE Transactions on Automatic Control, **46** (2001), 1447–1451.

[30] S. Tang, Z.Q. Zheng, and S.K. Qian: Nonlinear system identification of a small-scale unmanned helicopter. *Control Engineering Practice*, **25** (2014), 1–15.